ISSN 1063-7834, Physics of the Solid State, 2009, Vol. 51, No. 2, pp. 409–416. © Pleiades Publishing, Ltd., 2009.
Original Russian Text © D.I. Tetelbaum, A.N. Mikhaylov, A.I. Belov, A.V. Ershov, E.A. Pitirimova, S.M. Plankina, V.N. Smirnov, A.I. Kovalev, R. Turan, S. Yerci, T.G. Finstad, S. Foss, 2009, published in Fizika Tverdogo Tela, 2009, Vol. 51, No. 2, pp. 385–392.

LOW-DIMENSIONAL SYSTEMS AND SURFACE PHYSICS

Properties of Al_2O_3 : nc-Si Nanostructures Formed by Implantation of Silicon Ions into Sapphire and Amorphous Films of Aluminum Oxide

D. I. Tetelbaum[a], A. N. Mikhaylov[a], A. I. Belov[a], A. V. Ershov[a], E. A. Pitirimova[a], S. M. Plankina[a], V. N. Smirnov[a], A. I. Kovalev[b], R. Turan[c], S. Yerci[c], T. G. Finstad[d], and S. Foss[d]

[a] *Physico-Technical Research Institute of University of Nizhny Novgorod, pr. Gagarina 23/3, Nizhny Novgorod, 603950 Russia*
e-mail: tetelbaum@phys.unn.ru
[b] *Surface Phenomena Researches Group, CNIICHERMET, Vtoraya Baumanskaya ul. 9/23, Moscow, 105005 Russia*
[c] *Middle East Technical University, Ankara, Turkey*
[d] *University of Oslo, Blindern, Norway*

Received March 6, 2008; in final form, June 9, 2008

Abstract—Photoluminescence, infrared Fourier spectroscopy, Raman scattering, transmission electron microscopy, and electron diffraction were used to study the luminescent, optical, and structural properties of aluminum oxide layers (sapphire and films of Al_2O_3 deposited on silicon) implanted with Si^+ to produce silicon nanocrystals. It is established that, in both cases, a high-temperature annealing of heavily implanted samples brings about the formation of silicon nanocrystals. However, the luminescent properties of the nanocrystals are strongly dependent on the type of pristine matrix; namely, nanocrystals in Al_2O_3 films emit light in the spectral range typical of Si quantum dots (700–850 nm), whereas in sapphire this photoluminescence is not observed. This difference is interpreted as being due to the fact that local stresses arise in the nanocrystal/sapphire system and break chemical bonds at the interface between the phases, whereas in Al_2O_3 films stresses are relaxed.

PACS numbers: 78.55.Qr, 61.82.Rx, 68.55.Ln, 85.40.Ry, 78.55.Ap, 78.55.Qr, 78.30.Am, 68.37.Lp

DOI: 10.1134/S1063783409020334

1. INTRODUCTION

Recently, increased attention has been paid to studying silicon-based materials that are promising for creating next-generation opto- and nanoelectronic devices, such as light-emitting diodes, lasers, and memory cells [1, 2]. Integration of electronic and optical functions based on silicon planar technology would lead to radical advances in electronic engineering.

Bulk silicon has poor luminescence characteristics because it is an indirect-gap semiconductor, which hampers the development of effective silicon-based light-emitting structures and limits the application of Si in optoelectronics, in contrast to traditional microelectronics, where silicon dominates. One of the most effective ways to solve this problem is to form Si nanocrystals (NCs) in wide-band-gap dielectric matrices. Si NCs exhibit intense luminescence in visible (red) and infrared (IR) spectral ranges owing to quantum confinement, which makes it possible to increase the effective band gap width and enhance the radiative recombination probability.

Most research attention has been concentrated on silicon NCs in a silicon dioxide matrix (SiO_2 : nc-Si) forming upon decomposition of a supersaturated SiO_2 : Si solid solution [3–5]. The most appropriate method for producing such a system is ion implantation, which is compatible with the modern planar microelectronic technology. The properties of other nanocompositions containing Si NCs are much less understood.

An important factor determining the properties of Si NCs is the set of properties of the dielectric matrix in which the NCs are synthesized. From the fundamental viewpoint, it is important to elucidate how the change in the composition or type of matrix influences the regularities of formation and the properties of NCs. Moreover, by combining specific properties of a matrix and Si NCs, one can extend functional capabilities of nanomaterials produced.

In this respect, the use of aluminum oxide Al_2O_3 in the form of sapphire or amorphous films as a matrix is of particular interest. Single-crystal sapphire wafers have been used successfully in fabricating silicon-on-sapphire structures, which possess important advantages, such as radiation hardness. Owing to their high permittivity, amorphous Al_2O_3 films have been proposed as substitutes for silicon oxide used to form extremely thin dielectric layers underneath the gate in the technology of metal–oxide–semiconductor struc-

tures [6]. Also, the band structure of the Al_2O_3 : nc-Si system favors the quantum confinement of carriers.

The studies devoted to the Al_2O_3 : nc-Si system are few in number. Si NCs in amorphous and crystalline Al_2O_3 layers were produced using ion implantation [7–11], laser ablation [12, 13], and codeposition [14, 15] followed by annealing at 300–1100°C. It has been established that annealing an Al_2O_3 : Si solid solution brings about its decomposition and the formation of Si nanocrystallites, which were detected using electron microscopy and X-ray diffraction [7–10]. Upon annealings at temperatures of up to 900°C, Al_2O_3 matrices remained amorphous. At higher temperatures, in the case where ion implantation of Si into sapphire was used, irradiated layers were recrystallized, with Si NCs being oriented relative to the matrix [7–10]. However, to the best of our knowledge, these are no comparative studies (under identical conditions) of the properties of the Al_2O_3 : nc-Si system obtained using different forms of the ionic oxide, which would make it possible to elucidate the role played by the initial state of the matrix. This is important for obtaining Al_2O_3 : nc-Si that exhibits luminescence characteristic of Si NCs.

In this work, we conducted a comprehensive study of the luminescent and optical properties and the structure of layers obtained by ion implantation of silicon into sapphire wafers or amorphous Al_2O_3 films deposited on silicon. The dose of Si^+ ions and the annealing temperature are varied in wide ranges, and the evolution of the photoluminescence (PL) spectra is studied associated with both matrix defects and Si NCs formed.

2. EXPERIMENTAL TECHNIQUE

The pristine aluminum oxide is used in the form of (0001)-oriented single-crystal sapphire (α-Al_2O_3) wafers and amorphous Al_2O_3 films 300 nm thick deposited on silicon substrates. The films are deposited by electron-beam evaporation of cold-pressed Al_2O_3 pellets in a modernized commercial BU-1A setup. Implantation of 100-keV Si^+ ions to doses ranging from 5×10^{16} to 3×10^{17} cm^{-2} is performed in the ILU-200 setup. The average projected range of Si^+ ions in Al_2O_3 as calculated using the TRIM code [16] is ~95 nm. During irradiation, the temperature of samples does not exceed 50°C for a maximum current density of 5 $\mu A/cm^2$. The subsequent annealing is performed in a dried-nitrogen flow at temperatures ranging from 500 to 1100°C for 2 h.

The PL is excited by a pulsed nitrogen laser with a wavelength of 337 nm and measured at room temperature in the wavelength range 350–900 nm using an SP-150 monochromator (Stanford Research Systems) and an R928 photomultiplier (Hamamatsu). IR Fourier spectroscopy studies are conducted on a Varian Digi-Lab FTS-7000 spectrometer with a spectral resolution of 4 cm^{-1}. The Raman spectra are recorded on a LabRam confocal micro-Raman setup (Jobin Yvon) using the 632.8-nm line of a helium–neon laser for excitation. The scattered radiation is detected by a CCD camera in backscattering geometry. Reflection electron diffraction is studied on an ÉMR-102 setup with an accelerating voltage of 50 kV. Cross-section transmission electron microscopy studies are conducted using a TEM JEOL 2010F microscope at an energy of 200 keV, with an electron beam being focused on a sample surface area ~100 nm in diameter.

3. RESULTS AND DISCUSSION

The PL in the spectral range 350–900 nm is measured at room temperature at all steps of implantation and annealing. Figures 1a and 1b show the PL spectra of sapphire samples and amorphous Al_2O_3 films implanted with Si^+ to a dose of 10^{17} cm^{-2} and then annealed at various temperatures. Let us first discuss the PL in the short-wavelength range 400–500 nm. The PL band at ~400 nm is associated with oxygen-deficient centers, which represent an oxygen vacancy that captured two electrons (F center) [17]. The band at ~500 nm is due to aggregation of these defects forming F_2 centers (oxygen divacancies) [17].

It can be seen from Fig. 1 that, during implantation and annealing, these centers exhibit both common and different features in sapphire and Al_2O_3 films. First, these bands are more pronounced for the films, which is likely due to a larger oxygen deficiency in comparison with sapphire, a feature associated with the technique by which they were prepared. Second, in films, in contrast to sapphire, implantation does not quench the F-center band completely and enhances the F_2-center band. In irradiated films, the F and F_2 centers also remain after annealing at temperatures up to 1100°C and their PL increases in intensity with increasing dose up to 10^{17} cm^{-2}. This specific feature (in comparison with sapphire) can be due to the looser film structure (the presence of pores). Irradiation causes a partial dissociation of the oxide. In sapphire, the unbound oxygen formed can escape from the sample only through the surface, whereas in a film it can also penetrate into pores, which hampers the reverse process (stoichiometry recovery) decreasing the concentration of oxygen-deficient centers during both irradiation and annealing. Thus, in the films, the PL associated with oxygen-deficient centers is more pronounced and exhibits a different behavior upon irradiation and annealing than in sapphire.

It is seen from Fig. 1b that irradiation of films decreases the ratio of the F- and F_2-center band intensities. This effect can be radiation-stimulated merging of oxygen monovacancies into divacancies because ion

irradiation increases the mobility of point defects (through "radiation shaking") [18].

The broad PL band at 400–650 nm ("green band") observed in sapphire implanted and then annealed at 700°C was assumed to be associated either with aggregate *F* centers [11] or with "non-phase" Si inclusions (chains, rings, or fractal-like objects without phase boundaries) [19]. The formation of such inclusions has been observed during the decomposition of a Si solid solution in SiO_2 [19–22]. The latter assumption is more probable because this band is much broader than that corresponding to F_2 centers (Figs. 1a, 1b). This assumption is also confirmed by the fact that the behavior of this band with variations in the annealing temperature and implantation dose is similar to that of the band corresponding to non-phase inclusions in SiO_2 [19–22]; specifically, its intensity varies nonmonotonically with annealing temperature (reaching a maximum at the annealing temperature of 700°C) and Si^+ dose. This behavior can be associated with the gradual transformation of the non-phase inclusions formed during the annealing into "compact" Si inclusions [19, 20].

The most interesting result is that, after annealing at a high temperature (1100°C), the amorphous Al_2O_3 films exhibit "red" luminescence in the range 700–850 nm, which is typical of Si NCs in SiO_2 [3, 5]. This luminescence is not observed in sapphire. Let us discuss the behavior of this PL with variations in the regimes of implantation and annealing in order to elucidate its origin. Figure 1c shows the dose dependences of the intensity and peak position of the red PL of Al_2O_3 films annealed at 1100°C. It can be seen that the dose dependence of the intensity is nonmonotonic, with a maximum at $(1–2) \times 10^{17}$ cm^{-2}. An analogous behavior was observed for the PL associated with quantum confinement of carriers in Si NCs produced by ion implantation in thermal SiO_2 films [3, 5, 23, 24], which was explained by the increase of Si NCs in number in the initial range of the dose dependence and by their coalescence and increase in size in the range where the PL intensity decreases. The relation of the PL to radiative transitions between energy levels in quantum dots is confirmed by the shift in the PL peak position observed with variation in quantum-dot size [25].

In our case, the variation in the position of the red-PL peak with silicon dose (Fig. 1c) correlates with the variation in the PL intensity, as would be expected [3, 23]. Here, in contrast to the SiO_2 : nc-Si system [3, 23], the wavelength corresponding to the PL peak decreases somewhat with increasing dose in the initial range of the dose dependence (where the PL intensity increases), which indicates a decrease in the average NC size [25]. This difference is likely caused by the different kinetics of Si inclusion formation in an Al_2O_3 : Si solid solution. With increasing dose (Si concentration in the solid solution), the degree of supersaturation increases, which causes an increase in the formation rate of Si-phase inclusions and, hence, in their amount. The nucleation rate is a quadratic function of the Si concentration [5], whereas the concentration of the excess Si is proportional to the dose. Therefore, the number of Si atoms per nucleation center (for the same fraction of the silicon

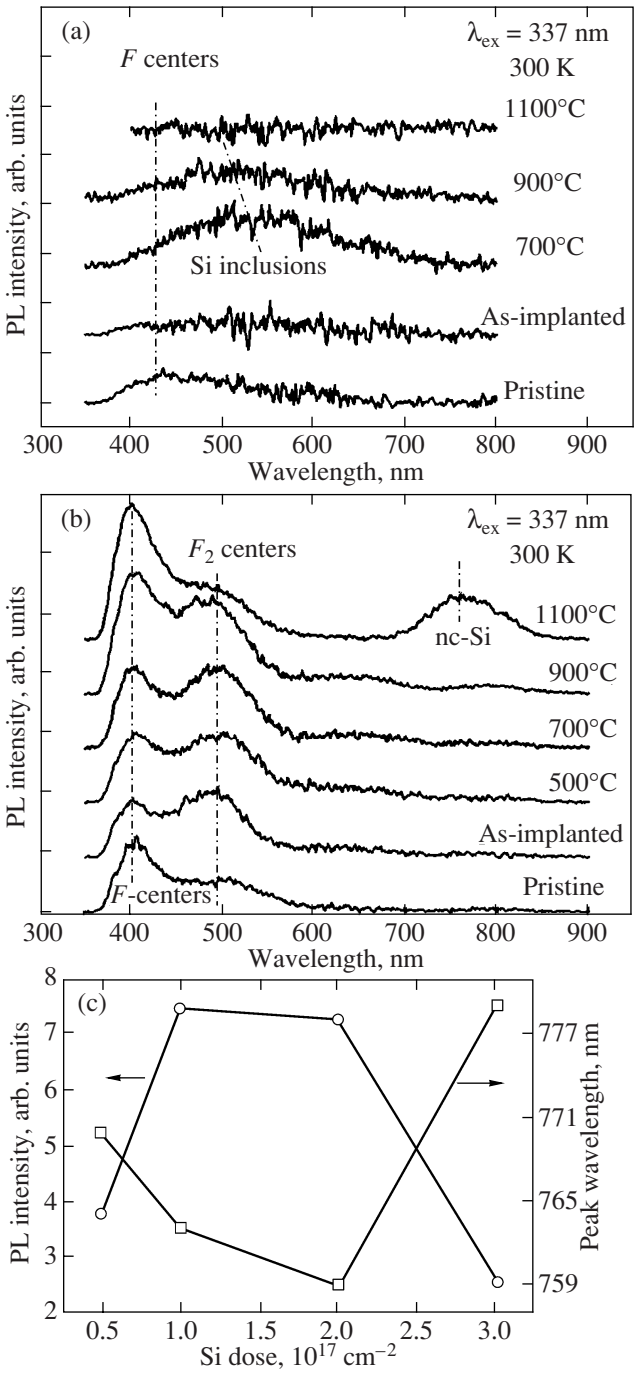

Fig. 1. (a, b) Effect of Si implantation (at a dose of 10^{17} cm^{-2}) and subsequent annealing on the PL spectra of (a) sapphire and (b) an amorphous Al_2O_3 film; (c) the dose dependences of the PL intensity and the PL peak position in the range 700–800 nm for implanted Al_2O_3 films after annealing at 1100°C.

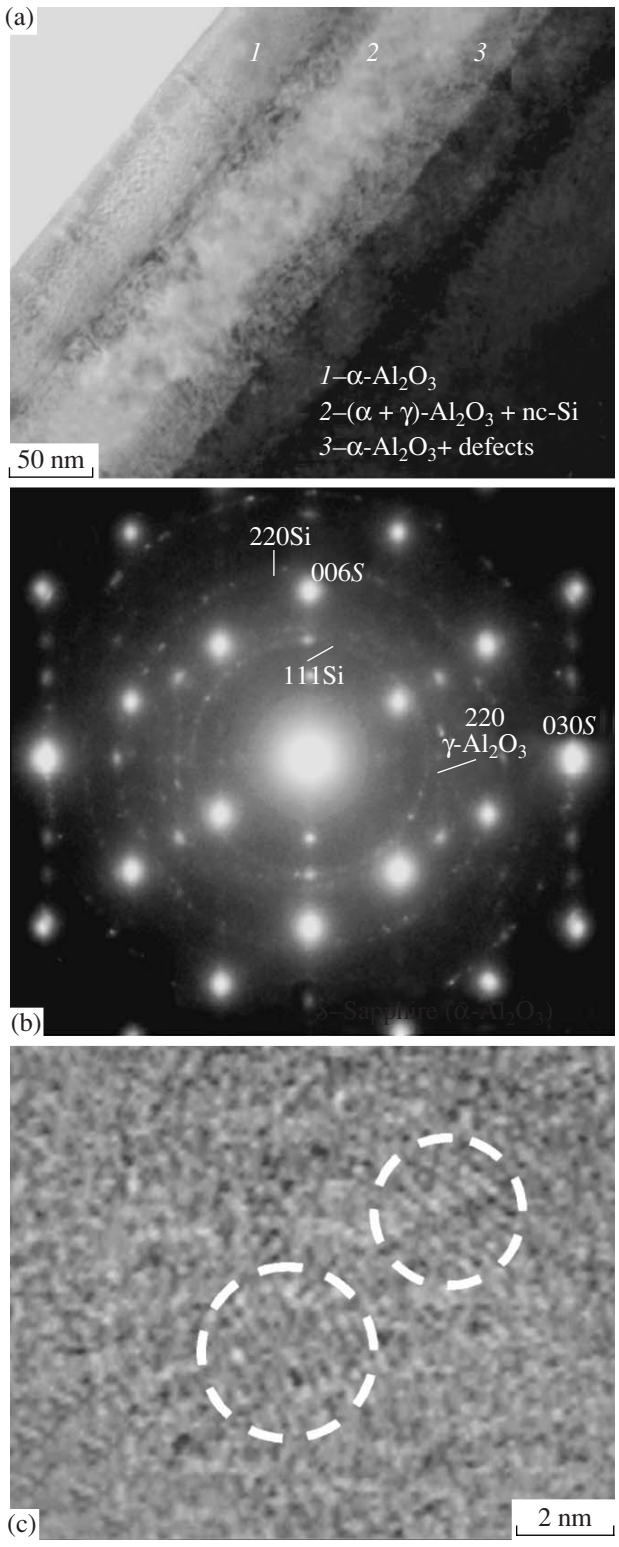

Fig. 2. (a) Transition electron microscopy image and (b) the electron diffraction pattern of a sapphire layer implanted by Si^+ ions (at a dose of 10^{17} cm^{-2}) and then annealed at 1050°C; (c) the high-resolution electron microscopy image of Si NCs in an amorphized Al_2O_3 layer after annealing at 700°C. In panel (b), *S* stands for sapphire (α-Al_2O_3).

going to form NCs) decreases and the NC size also decreases. Obviously, the fraction of the implanted silicon forming NCs and its variation with dose can depend on the matrix type. Therefore, it is no surprise that the situation in Al_2O_3 differs from that in SiO_2. The decrease of NCs in size can be caused by partial oxidation of Si NCs in the presence of a large amount of weakly bound oxygen in a deposited Al_2O_3 film and by the crystallization of the oxide matrix that occurs simultaneously with the formation of Si NCs (see below). The heterogeneous NC nucleation on oxide crystallites and the attendant increase of NCs in number at a fixed Si concentration should also decrease the average NC size. The decrease in the PL intensity and the increase in the radiation wavelength from ~760 to ~780 nm at large Si doses are consistent with the assumption that the average NC size increases due to coalescence, as observed in the SiO_2 : nc-Si system [23, 24].

Thus, the luminescent properties of Si NCs are dependent on the type of pristine Al_2O_3 matrix; namely, in Al_2O_3 films, the NCs emit light in the spectral range typical of them (as in the case of a SiO_2 matrix), whereas in implanted sapphire this PL is absent. It is conceivable that Si NCs do not form in implanted sapphire at all. However, this is not the case. We detected Si NCs using high-resolution electron microscopy (on a cross cleavage) and electron diffraction (Fig. 2). Implantation of Si ions brings about the formation of a buried amorphous layer (layer *2* in Fig. 2a), which is recrystallized at an annealing temperature of 900°C. The recrystallization is epitaxial and begins both on the substrate (layer *3*) and on the residual surface crystalline layer (layer *1*). During annealing at 1050°C, crystallization is almost fully completed, with γ-Al_2O_3 crystals being formed in addition to the initial α-Al_2O_3 phase. In all cases, after annealing (at least at 900°C or greater), the implanted layer contains randomly oriented Si crystallites ranging widely in size (10 ± 7 nm at 1050°C and a dose of 3×10^{17} cm^{-2}). It is established that γ-Al_2O_3 crystallites are orientationally matched with Si NCs and, therefore, are most likely to form through solid-state heteroepitaxial growth on the faces of Si NCs. The reverse situation, in which Si NCs grow on γ-Al_2O_3 particles that formed earlier, is also possible. The transition region between the recrystallized layer and the "substrate" (sapphire) is found to contain Si crystals epitaxially oriented relative to the pristine crystal. Therefore, it is reasonable to assume that Si NCs in annealed layers of implanted sapphire are subjected to stresses produced by the crystalline Al_2O_3 phase. The stresses are due to the difference between the equilibrium lattice parameters of the conjugated phases (Si and Al_2O_3), a phenomenon that is well known for gaseous-phase or molecular-beam epitaxy of silicon on sapphire. In our case, we deal, in essence, with the same phenomenon but on the nanoscopic rather than the macroscopic scale.

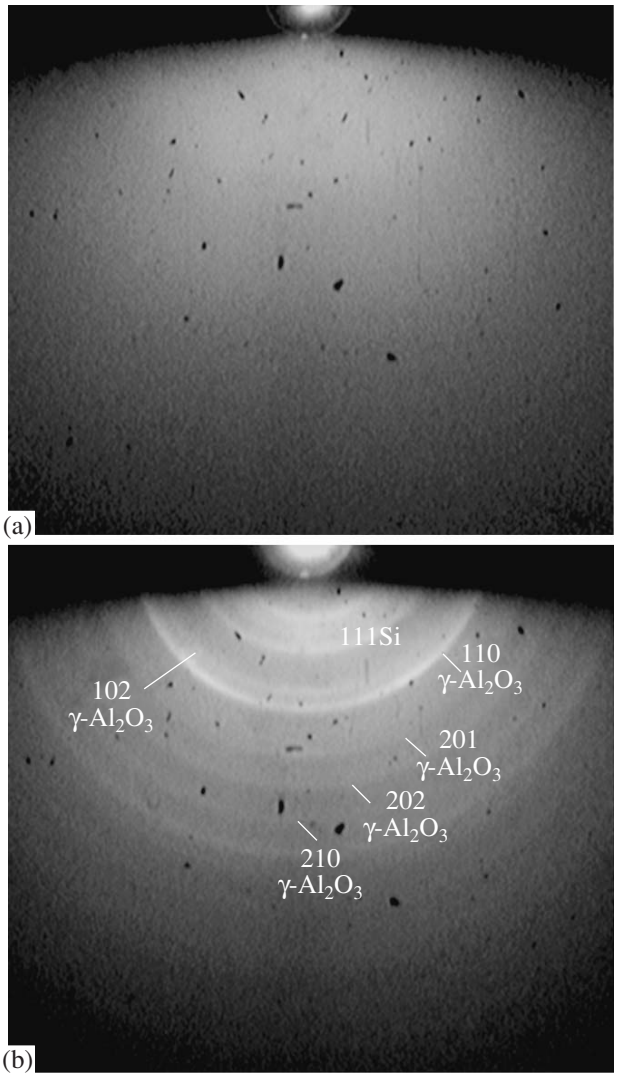

Fig. 3. Electron diffraction patterns of (a) a pristine Al_2O_3 film and (b) the film irradiated by Si^+ ions (at a dose of 3×10^{17} cm^{-2}) and then annealed at 1100°C.

In the case of ion implantation of amorphous Al_2O_3 films, the formation of Si NCs is confirmed by the reflection electron diffraction data. Figure 3a shows the electron diffraction pattern of a pristine Al_2O_3 film exhibiting a diffuse halo characteristic of the amorphous phase. After an annealing of an implanted film at 1100°C, its electron diffraction pattern (Fig. 3b) has a number of rings indicating that the film is partially crystallized. There is a ring corresponding to an interplanar spacing of 3.3 ± 0.1 Å, which is close to that of (111)Si (d = 3.12 Å), and rings corresponding to reflections (102), (110), (201), (202), and (210) of the γ-Al_2O_3 phase [26].

Important information concerning the phase composition of silicon-implanted layers of sapphire is obtained from the Raman spectroscopy data. Figure 4 shows the Raman spectra of sapphire samples irradiated by Si ions to a dose of 3×10^{17} cm^{-2} and then annealed at various temperatures. As in [11], these data indicate that crystalline Si inclusions form at annealing temperatures above 700°C. Indeed, these spectra contain narrow peaks whose position (520 cm^{-1} at 700°C, 522 cm^{-1} at 900°C, and 525 cm^{-1} at 1050°C) are close to that characteristic of bulk silicon (521 cm^{-1}). These peaks may be attributed to Si NCs. At annealing temperatures of 900°C and especially of 1050°C, the peaks are shifted to larger wavenumbers relative to that of bulk silicon. A decrease of crystals in size causes the frequency of scattered photons to shift to smaller wavenumbers. The shift in the opposite direction in our case indicates that the matrix exerts compressive stresses on NCs [11]. At annealing temperatures of 500–700°C, the spectra have broad bands with a maximum at 480–490 cm^{-1} corresponding to amorphous Si inclusions [22] and, perhaps, non-phase inclusions. We note that the green PL band (see above) is observed in the case where, according to the Raman spectroscopy data, a large fraction of implanted silicon forms noncrystalline Si inclusions. This confirms the above assumptions concerning the origin of this band.

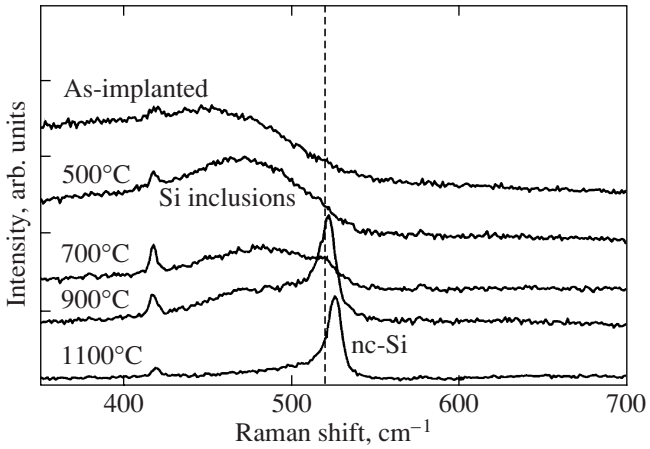

Fig. 4. Raman spectra of sapphire implanted by Si^+ ions (at a dose of 3×10^{17} cm^{-2}) and then annealed at various temperatures. The dashed line indicates the position of the scattering peak in bulk silicon.

Thus, the existence of Si NCs in sapphire layers implanted and then annealed at high temperatures is confirmed by the transmission electron microscopy, electron diffraction, and Raman spectroscopy data. However, these NCs do not exhibit the luminescent properties characteristic of Si quantum dots; namely, they do not emit light with wavelengths 700–850 nm. What is the reason for this and why is the Si nanocrystal PL band clearly observed when Si is implanted into amorphous films? From the above data, it follows that the main reason for the absence of Si nanocrystal PL in sapphire is stress and the breakage of bonds at the Si NC/Al_2O_3 interfaces caused by it. Stresses can arise, first, on cooling of the samples after annealing because

of the difference between the coefficients of thermal expansion of Si and sapphire [27] and, second, due to the coherent conjugation (dictated by the crystalline Al_2O_3 phase) between the lattice of Si NCs and that of the epitaxially recrystallized sapphire layer (according to the transmission electron microscopy data). Let us discuss the former mechanism.

In order to estimate the stress exerted on NCs by the matrix, we consider a sphere located in a cavity [28]. For simplicity, we assume that the spherical silicon inclusion is formed at an annealing temperature T_{ann} in an infinite isotropic sapphire matrix.

Let V_0 be the volume of the spherical cavity in sapphire and the volume of the Si inclusion immediately after an annealing at a temperature T_{ann}. The stress acting on the inclusion is zero at this instant of time. During cooling from T_{ann} to room temperature (T_r), the volumes of the cavity and inclusion change and stresses arise due to the difference between the volume expansion coefficients of the matrix and inclusion. Following the procedure described in [28], we mentally remove the Si inclusion from the cavity in sapphire and determine the change in their volumes (ΔV_{free}^{Si} and ΔV_{free}^{S}) when they are cooled independently in the free state

$$\frac{\Delta V_{free}^{Si}}{V_0} = \left(\frac{V_1^{Si} - V_0}{V_0}\right) = \beta_V^{Si}(T_r - T_{ann}), \quad (1a)$$

$$\frac{\Delta V_{free}^{S}}{V_0} = \left(\frac{V_1^{S} - V_0}{V_0}\right) = \beta_V^{S}(T_r - T_{ann}), \quad (1b)$$

where V_1^{Si} and V_1^{S} are the volumes of the Si inclusion and the cavity in sapphire after cooling to T_r, respectively, and β_V^{Si} and β_V^{S} are the volume expansion coefficients of silicon and sapphire (in our case, $\beta_V^{Si} < \beta_V^{S}$). Then, we put the inclusion back into the cavity. Let V_{dis} be the disparity between the inclusion volume V_1^{Si} and the cavity volume V_1^{S} before the inclusion is put into the cavity,

$$V_{dis} = V_1^{Si} - V_1^{S}. \quad (2)$$

Denoting the changes in the volumes of the cavity and inclusion caused by the placement of the inclusion in the cavity by ΔV_C^{S} and ΔV_C^{Si}, respectively, and using the relation $V_{dis} = \Delta V_C^{S} - \Delta V_C^{Si}$, we find that [28]

$$\Delta V_C^{S} = \frac{V_{dis}}{\gamma'}, \quad \gamma' = \frac{3K^{Si} + 4\mu^{S}}{3K^{Si}}, \quad (3)$$

where K^{Si} is the bulk modulus of Si and μ^{S} is the shear modulus of sapphire.

Knowing V_{dis} and ΔV_C^{S}, we can find the change in volume ΔV_C^{Si}, which is the volume deformation of the Si inclusion in the cavity caused by cooling

$$\Delta V_C^{Si} = \Delta V_C^{S} - V_{dis}. \quad (4)$$

According to the Hook law, the stress σ acting on the inclusion is

$$\sigma = K^{Si}\frac{\Delta V_C^{Si}}{V_0}. \quad (5)$$

We use the volume expansion coefficients of Si and Al_2O_3 [27] averaged over the temperature range from T_{ann} to T_r and also $K^{Si} = 100.75 \times 10^9$ Pa [27] and $\mu^{S} = 1.57 \times 10^{11}$ Pa.

For an annealing temperature of 1050°C, the stress is calculated to be $\sigma \approx -8 \times 10^8$ Pa. We note that, in [11], based on the Raman scattering data, the stress was estimated to be on the order of 10^9 Pa for analogous regimes of implantation and annealing. Thus, Si NCs in a sapphire matrix are subjected to stresses close to the ultimate stress for silicon, $\sigma_{max} = 7 \times 10^8$ Pa [27]. Such large stresses can bring about the formation of dangling bonds (nonradiative recombination centers) at the NC/matrix interfaces.

Another possible reason for stresses is the lattice mismatch of phases mentioned above. However, a correct calculation for this case is complicated and ambiguous, because it requires that the stress relief caused by point and extended defects during NC formation be taken into account.

As mentioned above, ion implantation of amorphous Al_2O_3 films on a Si substrate, in contrast to that of sapphire, brings about the appearance of a PL band at 700–850 nm, which is typical of Si NCs. Perhaps, relaxation of stresses in films deposited on silicon is favored by less strong adhesion to the substrate (in comparison with the irradiated sapphire layer) and by the looser film structure (the presence of pores).

Another factor distinguishing Al_2O_3 films from sapphire is the presence of excess oxygen mentioned above, which causes the oxidation of the Si NC/matrix interfaces during annealing. Figure 5 shows the IR Fourier spectroscopy data for Al_2O_3 films irradiated by Si^+ ions to a dose of 3×10^{17} cm^{-2} and then annealed at various temperatures. It can be seen that there are absorption bands near 550 and 735 cm^{-1} associated with vibrations of Al–O bonds [15]. The intensity of these bands increases with annealing temperature, which can be interpreted as being due to the recovery of stoichiometry and the ordering of the Al_2O_3 phase during annealing. An annealing at a high temperature causes the appearance of additional absorption bands at 460, 810, and 1080 cm^{-1}. According to [29], these bands are associated with various vibration modes of Si–O–Si bonds

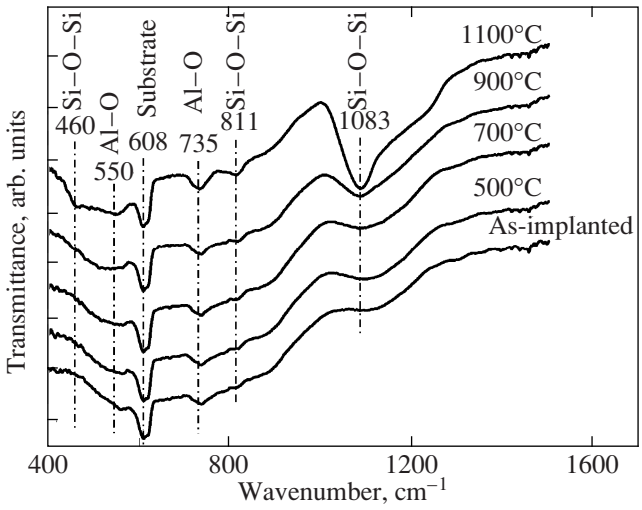

Fig. 5. IR transmission spectra of Al_2O_3 films irradiated by Si^+ ions (at a dose of 3×10^{17} cm^{-2}) and then annealed at various temperatures.

in silicon oxide. The fact that the intensity of these bands increases significantly with Si dose indicates that Si–O–Si bonds are formed inside the silicon-implanted Al_2O_3 layer rather than at the interface between Al_2O_3 and the silicon substrate. The band at 1080 cm^{-1} is close in frequency to a nonsymmetric stretching vibration mode in SiO_2 [29], which indicates that the Si–O–Si bonds belong to the SiO_x phase rather than to complexes (dispersed in the Al_2O_3 matrix) that can be formed by implanted Si atoms binding with O atoms of the matrix. These data can be explained assuming that Si NCs are surrounded by SiO_2 or SiO_x shells [15], which favor stress relief. All these factors account for the difference between the mechanical properties of NCs in sapphire and in Al_2O_3 films.

4. CONCLUSIONS

We have performed a comparative analysis of the photoluminescence (PL) of Al_2O_3 layers (single-crystal sapphire and amorphous films) implanted by Si^+ ions and then annealed at various temperatures. We have revealed specific features of the PL associated with oxygen-deficient centers in oxide layers differing in nature and found significantly different manifestations of the PL of silicon nanoinclusions forming during phase separation in the Al_2O_3 : Si system. The data obtained by several methods of analyzing the structure and phase composition of implanted layers were used to interpret the PL regularities.

The implantation of Si ions into sapphire brings about the formation of a buried amorphous layer. During an annealing at a high temperature, this layer is epitaxially recrystallized with the formation of silicon nanocrystals (NCs) in it. The PL spectra exhibit a band at ~550 nm associated with radiation emitted by noncrystalline silicon precipitates. However, the PL at 700–850 nm, which is typical of Si NCs, is not observed. The absence of this PL is likely caused by large stresses (~1 GPa), which bring about the formation of dangling bonds (nonradiative recombination centers) at the NC/matrix interfaces.

Si-implanted amorphous Al_2O_3 films, in contrast to implanted sapphire, exhibit the PL typical of Si NCs. It intensity depends nonmonotonically on Si dose, which is explained (as in the SiO_2 : nc-Si system) by an increase of NCs in number (in the dose range where the PL intensity increases) and their coalescence (in the dose range where the PL intensity decreases). The oxide matrix structure influences the formation of Si nanoinclusions and, hence, their luminescent properties.

Thus, not only the chemical nature of the matrix but also its initial state and preparation technique have a significant effect on the ability of Si NCs to emit light in the visible and infrared spectral ranges.

ACKNOWLEDGMENTS

This work was supported in part by project FP6 SEMINANO (contract NMP4-CT-2004-505285), the Ministry of Education and Science of the Russian Federation (RNP nos. 2.1.1.4022, 2.2.2.2.4737, 2.2.2.3.10002), CRDF (BRHE REC-001, Y4-P-01-05), RFBR (project no. 05-02-16762), and the Council on Grants from the President of the Russian Federation (grant MK-3877.2007.2).

REFERENCES

1. P. Bettotti, M. Cazzanelli, L. Dal Negro, B. Danese, Z. Gaburro, C.J. Oton, G. Vijaya Prakash, and L. Pavesi, J. Phys.: Condens. Matter **14**, 8253 (2002).
2. L. Pavesi, Mater. Today **1**, 18 (2005).
3. T. Shimizu-Iwayama, S. Nakao, and K. Saitoh, Appl. Phys. Lett. **65**, 1814 (1994).
4. B. Garrido, M. Lopez, A. Perez-Rodriguez, C. Garcia, P. Pellegrino, R. Ferre, J. A. Moreno, J. R. Morante, C. Bonafos, M. Carrada, A. Claverie, J. de la Torre, and A. Souifi, Nucl. Instrum. Methods Phys. Res., Sect. B **216**, 213 (2004).
5. D. I. Tetelbaum, A. N. Mikhaylov, O. N. Gorshkov, A. P. Kasatkin, A. I. Belov, D. M. Gaponova, and S. V. Morozov, Vacuum **78**, 519 (2005).
6. G. D. Wilk, R. M. Wallace, and J. M. Anthony, J. Appl. Phys. **89**, 5243 (2001).
7. C. J. Park, Y. H. Kwon, Y. H. Lee, T. W. Kang, H. Y. Cho, S. Kim, S.-H. Choi, and R. G. Elliman, Appl. Phys. Lett. **84**, 2667 (2004).
8. D. I. Tetelbaum, O. N. Gorshkov, A. V. Ershov, A. P. Kasatkin, V. A. Kamin, A. N. Mikhaylov, A. I. Belov, D. M. Gaponova, L. Pavesi, L. Ferraioli, T. G. Finstad, and S. Foss, Thin Solid Films **515**, 333 (2006).

9. C. W. White, J. D. Budai, S. P. Withrow, S. J. Pennycook, D. M. Hembree, D. S. Zhou, T. Vo-Dinh, and R. H. Magruder, Mater. Res. Soc. Symp. Proc. **316**, 487 (1994).
10. S. Yanagiya and M. Ishida, J. Electron. Mater. **28**, 496 (1999).
11. S. Yerci, U. Serincan, I. Dogan, S. Tokay, M. Genisel, A. Aydinli, and R. Turan, J. Appl. Phys. **100**, 074 301 (2006).
12. Y. Zhu and P. P. Ong, Surf. Rew. Lett. **8**, 559 (2001).
13. P. P. Ong and Y. Zhu, Physica E (Amsterdam) **15**, 118 (2002).
14. Q. Wan, C. L. Lin, W. L. Liu, and T. H. Wang, Appl. Phys. Lett. **82**, 4708 (2003).
15. L. Bi and J. Y. Feng, J. Lumin. **121**, 95 (2006).
16. J. F. Ziegler, J. Appl. Phys. **85**, 1249 (1999).
17. B. D. Evans, G. J. Pogatshnik, and Y. Chen, Nucl. Instrum. Methods Phys. Res., Sect. B **91**, 258 (1994).
18. V. L. Indenbom, Pis'ma Zh. Tekh. Fiz. **5** (4), 489 (1979) [Sov. Tekh. Phys. Lett. **5** (4), 200 (1979)].
19. G. A. Kachurin, A. F.Leier, K. S. Zhuravlev, I. E. Tyschenko, A. K.Gutakovskii, V. A. Volodin, V. Skorupa, and R. A. Yankov, Fiz. Tekh. Poluprovodn. (St. Petersburg) **32** (11), 1371 (1998) [Semiconductors **32** (11), 1222 (1998)].
20. L. X. Yi, J. Heitmann, R. Scholz, and M. Zacharias, Appl. Phys. Lett. **81**, 661 (2002).
21. P. Mutti, G. Ghislotti, S. Bertoni, L. Bonoldy, G. F. Cerofolini, L. Meda, E. Grilli, and M. Guzzi, Appl. Phys. Lett. **66**, 851 (1995).
22. G. A. Kachurin, S. G. Cherkova, V. A. Volodin, D. V. Marin, and M. Deutshmann, Fiz. Tekh. Poluprovodn. (St. Petersburg) **42** (2), 181 (2008) [Semiconductors **42** (2), 183 (2008)].
23. D. I.Tetelbaum, O. N. Gorshkov, A. P. Kasatkin, A. N.Mikhaylov, A. I. Belov, D. M. Gaponova, and S. V. Morozov, Fiz. Tverd. Tela (St. Petersburg) **47** (1), 17 (2005) [Phys. Solid State **47** (1), 13 (2005)].
24. Y. Q. Wang, R. Smirani, and G. G. Ross, Nano Lett. **4**, 203 (2004).
25. V. A. Burdov, Fiz. Tekh. Poluprovodn. (St. Petersburg) **36** (10), 1233 (2002) [Semiconductors **36** (10), 1154 (2002)].
26. L. I. Mirkin, *Handbook of X-Ray Analysis of Polycrystalline Materials* (Fizmatlit, Moscow, 1961; Plenum, New York, 1964).
27. *Handbook of Physical Quantities*, Ed. by I. S.Grigoriev and E. Z. Meilikhov (Énergoatomizdat, Moscow, 1991; CRC Press, Boca Raton, FL, United States, 1996).
28. D. Eshelby, in *Solid State Physics*, Ed. by F. Seitz and D. Turnbull (Academic, New York, 1956; Inostrannaya Literatura, Moscow, 1963), Vol. 3.
29. C. T. Kirk, Phys. Rev. B: Condens. Matter **38**, 1255 (1988).

Translated by Yu. Epifanov